Computers & Industrial Engineering 82 (2015) 41–53

Contents lists available at ScienceDirect

Computers & Industrial Engineering

journal homepage: www.elsevier.com/locate/caie

Three-dimensional variation propagation modeling for multistage turning process of rotary workpieces

Shichang Du [a,b,*], Xufeng Yao [c], Delin Huang [a], Meng Wang [a]

[a] Department of Industrial Engineering and Management, School of Mechanical Engineering, Shanghai Jiaotong University, Shanghai 200240, PR China
[b] State Key Lab of Mechanical System and Vibration, Shanghai 200240, PR China
[c] Department of Mechanical and Industrial Engineering, University of Illinois, Chicago, IL 60607, USA

ARTICLE INFO

Article history:
Received 27 February 2014
Received in revised form 7 January 2015
Accepted 9 January 2015
Available online 24 January 2015

Keywords:
Multistage turning process
Rotary workpiece
Variation propagation model
Differential motion vector
State space model

ABSTRACT

In spite of the success of state space modeling approach to describe variation propagation for multistage milling processes (MMPs), the current models cannot be directly applied into variation propagation analysis for multistage turning processes (MTPs) due to the differences of the locating datum schemes. MTPs are widely adopted in manufacturing industry for fabricating rotary workpieces. In this paper, a generic framework for three-dimensional variation propagation modeling for MTPs of rotary workpieces based on differential motion vectors (DMVs) is developed. The explicit three-dimensional datum error and fixture error expressions are derived. By a series of homogeneous transformations of different error sources, a three-dimensional variation propagation model for MTPs is built, in which the datum error, fixture error and so on are described and transmitted in six degrees of freedom. The effectiveness of the proposed model is validated by an example of MTPs of valve shell.

1. Introduction

The ability to reduce process variation for quality improvement in manufacturing process plays an essential role in the success of a manufacturing enterprise in today's globally competitive marketplace (Du, Xi, Ni, Pan, & Liu, 2008). Though statistical process control (SPC) technique has been widely used for monitoring process variation in many applications (Du, Huang, & Lv, 2013; Du & Lv, 2013; Du, Lv, & Xi, 2012), it could not be used as a tool for analysis of variation propagation in manufacturing process. The forming of complex workpieces involves a large number of machining stages. As workpieces move through these stages, the variations of the characteristics are introduced. If characteristics machined in upstream stages are used as datum in downstream stages, the variations will be transmitted to newly generated characteristics and accumulated to the final products. Therefore, the variations can be attributed to two categories: variations generated at the current stage, as well as the variations accumulated from previous stages. The variations of the final product are the accumulation of variations from all stages.

Variation propagation modeling and monitoring for multistage processes has received intensive investigation in the recent decades (Bai & Yun, 1996; Shetwan, Vilentin, & Tjahjono, 2011; Shi, 2006). The engineering model directly linking engineering knowledge of the process variation sources with key product characteristic (KPC) measurements has received great attention. Among all the engineering models, the state-space based model is an effective model, which can be generally divided into two categories, multistage assembly process (MAP) model and multistage milling process (MMP) model. The state space model for variation propagation was first proposed for two-dimensional assembly processes (Jin & Shi, 1999; Mantripragada & Whitney, 1999) and was further investigated and applied in three-dimensional assembly processes (Camelio, Hu, & Ceglarek, 2004; Ding, Ceglarek, & Shi, 2002). In assembly processes, the fixture re-orientation errors, workpiece fabrication errors, workpiece joint errors (such as lap-, butt-, mixed-joint errors) mainly cause the dimension variation propagation; while in machining process, locating datum errors and fixture errors couple together to make variation propagation quite complicate and are the main reasons why the variation propagates.

For MMP, some authors (Djurdjanovic & Ni, 2001; Huang & Shi, 2004a,b) investigated the three dimensional variation propagation at the systemic level by applying the state space model. Huang, Shi, and Yuan (2003) generalized the variation propagation model with an approximate linearization strategy. Zhou, Huang, and Shi (2003) developed a variation propagation model and derived explicit expression for datum error and fixture error. Huang and Shi (2004a,b) extended the state space modeling approach from single

* Corresponding author at: Department of Industrial Engineering and Management, School of Mechanical Engineering, Shanghai Jiaotong University, Shanghai 200240, PR China.

http://dx.doi.org/10.1016/j.cie.2015.01.010
0360-8352/

Nomenclature

Notation	
RCS	reference coordinate system
MCS	machine coordinate system
FCS\\$^0$FCS	actual (nominal) fixture coordinate system
LCS_n	nth local coordinate system
RCS(k)	RCS at stage k, always abbreviated as $R(k)$ or R
FCS(k)	FCS at stage k, always abbreviated as $F(k)$ or F
HTM	homogeneous transformation matrix
H_n^R ($^0H_n^R$)	actual (nominal) HTM from LCS_n to RCS
R_n^R	rotaional component in HTM form LCS_n to RCS
t_n^R ($^0t_n^R$)	the coordinate value of the origin of LCS_n with respect to RCS, $t_{nx}^R, t_{ny}^R, t_{nz}^R$ are the three elements of t_n^R
$\hat{t}_n^R$	Skew symmetric matrix composed by the three elements of t_n^R, similar to R_n^R
Q_n^R	coupling matrix computed by R_n^R and $\hat{t}_n^R$
n_n^R, o_n^R, a_n^R	the column vector R_n^R
Δ_n^R ($\bar{\Delta}_n^R$)	differential transmission matrix from LCS_n to RCS, and its inverse matrix
$\hat{\theta}_n^R$	skew symmetric matrix of Δ_n^R composed by its three angular components
θ_n^R	a vector composed by the three angular components of $\hat{\theta}_n^R$, that is $(\theta_{nx}^R, \theta_{ny}^R, \theta_{nz}^R)^T$
d_n^R	a vector composed by the three positional components of Δ_n^R,that is $(d_{nx}^R, d_{ny}^R, d_{nz}^R)$
p_i^F	the coordinate value of point i with respect to coordinate system F
$p_x^F p_y^F p_z^F$	three component of p_i^F
x_A^B	the differential motion vector, representing the deviation of characteristic A w.r.t coordinate system B.
$x_i^{R(k)}$	the deviation of the ith characteristic w.r.t. $R(k)$
$X_0(k)$	deviation of all characteristics at stage k after relocation
$X^{new}(k)$	stage error propagated at stage k
$X(k)$	deviation of all characteristics after the processing of stage k
$l(k)$	number of characteristics manufactured at stage k
$i(k)$	the ith characteristic manufactured at stage k
$u_f(k), u_t(k)$	fixture error and tool error
$u_s(k)$	stage error coupled by the tool error and fixture error
$u(k)$	the variation input of stage k, composed by $u_f(k)$ and $u_t(k)$
$w(k)$	system noises, includes the variation introduced by unconsidered variation sources

process route to a serial-parallel hybrid MMP with multiple routes. Loose, Zhou, and Ceglarek (2007) developed a variation propagation model for general fixture setup schemes. Loose, Zhou, Zhou, and Ceglarek (2010) integrated geometric dimensioning and tolerancing (GD&T) into dimensional variation models for MMP. Cao, Subramaniam, and Chen (2012) proposed a performance evaluation and enhancement method of MMPs with rework loops. Abellan-Nebot, Liu, Subirón, and Shi (2012) extended the state space model for MMP considering the machining-induced error. Detailed descriptions of existing research work on variation propagation modeling and applications were provided in a monograph (Shi, 2006) and a survey (Shi & Zhou, 2009).

However, the current state space models only investigate variation propagation for MMPs for fabricating cubic workpieces. Due to the difference of the variation propagation principle existing between in MMPs for fabricating cubic workpieces and in multistage turning processes (MTPs) for fabricating rotary workpieces, these models for MMPs cannot be directly applicable to MTPs (Du, Yao, & Huang, 2015). Fig. 1 shows the difference of the locating scheme between MMP and MTP. The left part of Fig. 1 shows the locating scheme of a typical cubic workpieces, the locating scheme of engine cylinder head; while the right part of Fig. 1 shows the locating scheme of a rotary workpiece.

MTPs are widely adopted in manufacturing industry for fabricating rotary workpieces. Due to the differences of reasons causing variation propagation and limited research, it is desirable to analyze and model the variation propagation for MTPs. Therefore, the purpose of this paper is to present a generic framework for three-dimensional variation propagation modeling for MTPs of rotary workpieces by developing the explicit three-dimensional expressions of datum error and fixture error.

The remainder of this paper is organized as follows: Section 2 derives the mathematic representations of datum error, fixture error and machining error. Section 3 presents the variation coupling analysis procedure. A generic variation propagation modeling framework for MTPs is developed in Section 4. The model is validated by the turning process of a valve shell in Section 5. Finally, the conclusions are given in Section 6.

2. Workpiece random geometric error representation

2.1. Coordinate system definition

Before deriving the expression of variations, four types of coordinate systems are defined as follows:

1. The reference coordinate system (RCS) is rigidly associated with an individual workpiece and it is used to represent the location and orientation of the workpiece, also called workpiece coordinate system.
2. The fixture coordinate system (FCS) defines the actual fixture setup that locates the workpiece and it is determined by the actual position of locators.
3. The nominal fixture coordinate system (^{0}FCS) defines the nominal fixture setup, and it is determined by the nominal position of each locators. The notion with left superscript 0 is used to describe the nominal condition. Since the ^{0}FCS is fixed on the machine, it can also be considered as the machine coordinate system (MCS).
4. The local coordinate system (LCS), which is fixed with characteristics on workpieces, represents the actual location and orientation of characteristics of the workpiece.

2.2. Error definition

Four types of errors are derived from the relationships of the aforementioned coordinate systems and are listed as follows.

1. Tool error is the deviation of the LCS with respect to ^{0}FCS.
2. The fixture error is the deviation of the actual FCS with respect to the nominal ^{0}FCS.
3. The datum error is the positional and angular inconformity of the actual RCS with respect to FCS, which is usually caused by the inaccurate positioning datum.
4. The overall characteristic error is the deviation of LCS with respect to RCS, representing the overall position and orientation deviation of characteristics of a workpiece.

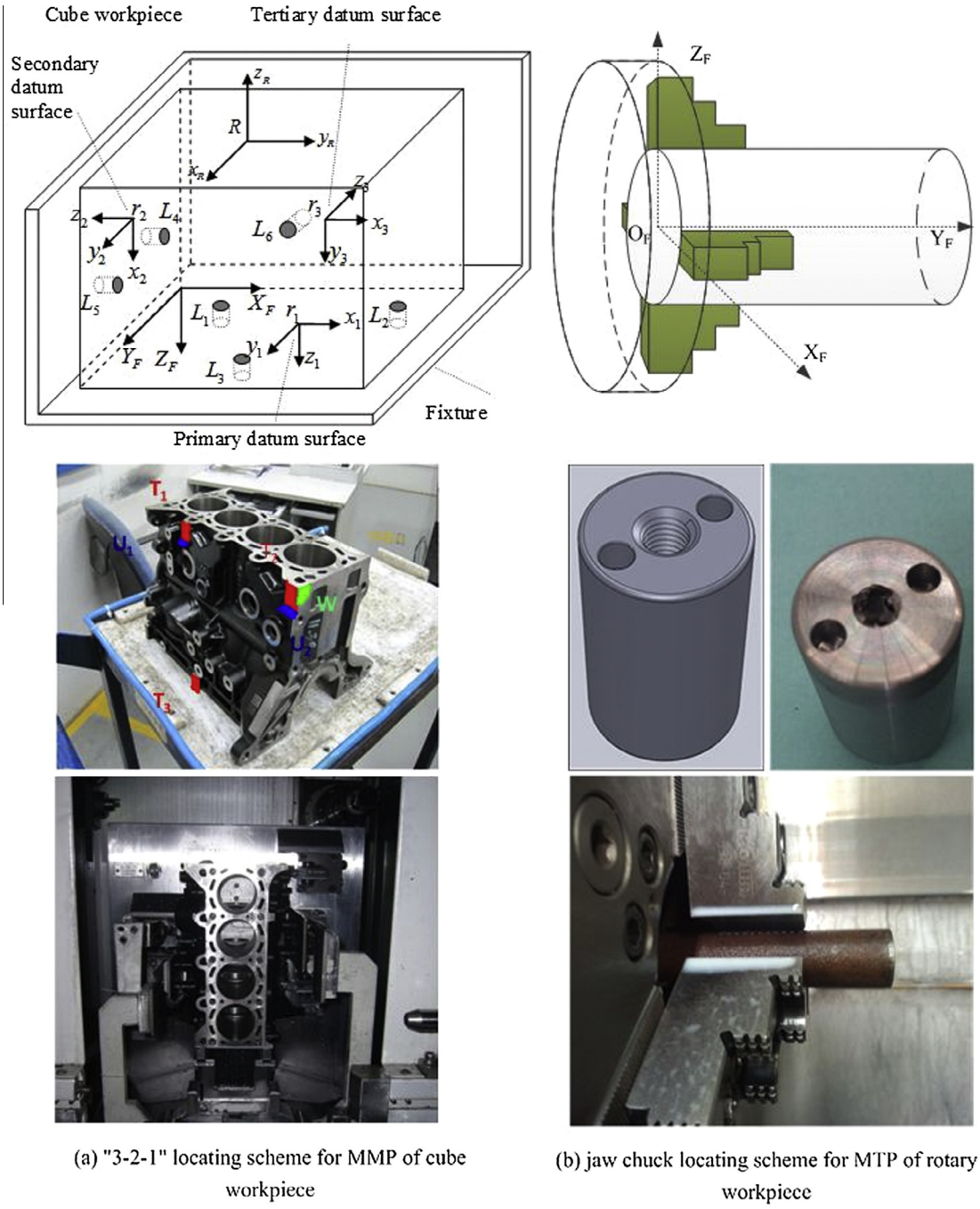

(a) "3-2-1" locating scheme for MMP of cube workpiece

(b) jaw chuck locating scheme for MTP of rotary workpiece

Fig. 1. Difference of locating scheme between MMP and MTP.

All the coordinate systems and their relationships are illustrated as Fig. 2.

2.3. Characteristic and variation representation

A characteristic of a workpiece is depicted by its location, orientation and size. In this paper, differential motion vectors (DMV) is adopted as state vector to represent the location and orientation variations of a characteristic. According to Section 2.1, the relationship between the FCS and RCS can be used to illustrate the location and orientation of a characteristic of workpiece. In Fig. 3, a cylinder characteristic is shown, and its location is represented by the location of a specific point O_i, the orientation of the characteristic is depicted by the rotational degree between coordinate $X_i|X_R$, $Y_i|Y_R$ and $Z_i|Z_R$, and its size is represented by the diameter and depth of the cylinder. The characteristic is represented by its location and orientation: $(x_i, y_i, z_i, \alpha, \beta, \gamma)$, where (x_i, y_i, z_i) are the location of point T in $O_RX_RY_RZ_R$, and (α, β, γ) is the rotational degree of transforming coordinate system $O_iX_iY_iZ_i$ to coordinate system $O_RX_RY_RZ_R$.

The vectorial dimensioning tolerancing (VD&T) representation is the aggregation of the position and orientation information of a characteristic (Loose et al., 2010). It contains the characteristic's six degree of freedoms. The variation of a characteristic in the turning process is reflected by its changes of location and orientation in six degree of freedoms and noted as:

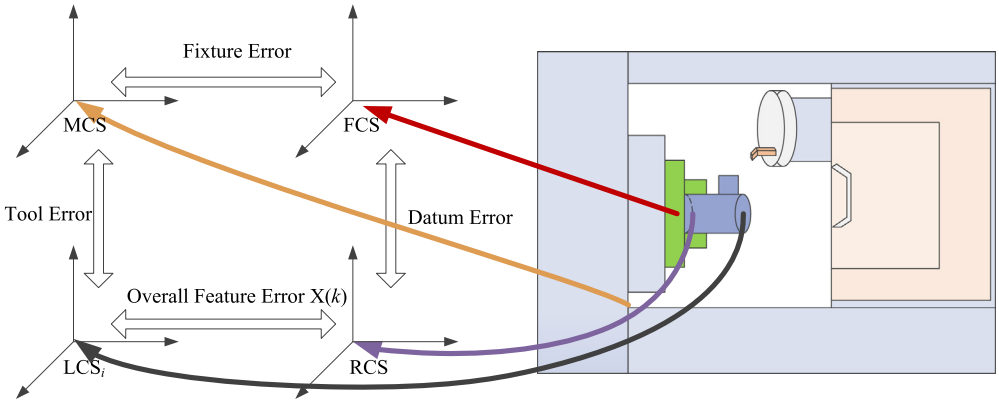

Fig. 2. Illustration of coordinate system and error.

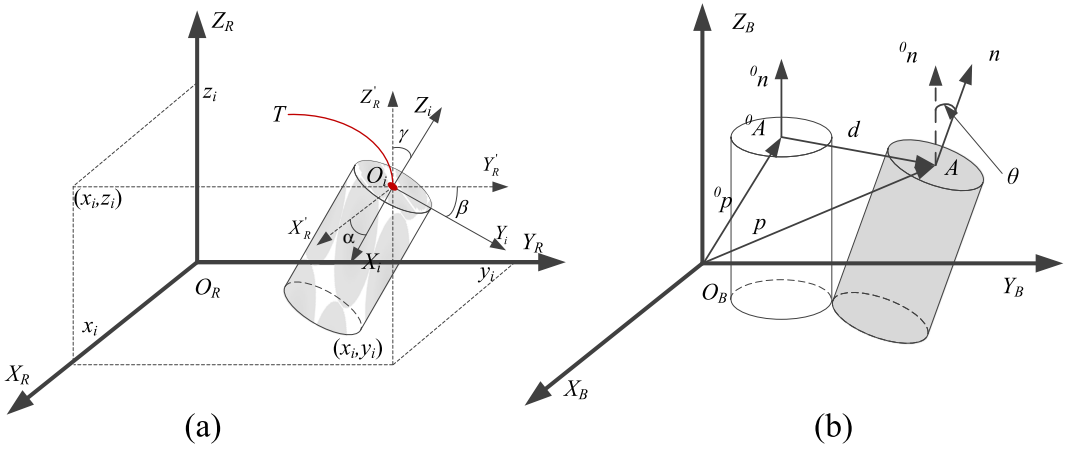

Fig. 3. Feature and deviation representation.

$$x_A^B = \left[\left(d_A^B\right)^T \quad \left(\theta_A^B\right)^T\right]^T q \tag{1}$$

where $d_A^B = \left[d_{Ax}^B \quad d_{Ay}^B \quad d_{Az}^B\right]^T$ is the positional error, and $\theta_A^B = \left[\theta_{Ax}^B \quad \theta_{Ay}^B \quad \theta_{Az}^B\right]^T$ is rotational error.

3. Variation coupling analysis

The DMV cannot be directly applied to basic arithmetic operations such as addition and subtraction, because of the Euler angles it contains. In order to conduct variation coupling analysis, a new set of rule is established for DMV calculation in this section.

3.1. Rotation and translation matrix

Before introducing the transformation matrix, two components of the transformation matrix are firstly introduced as follows:

3.1.1. Rotation matrix

Note $Rot(k, \theta)$ as the rotation matrix for the operation of rotating an object around axis k for a degree θ. Assume that a point has a coordinate (x, y, z) in the original coordinate system (representing the position and orientation of the object before rotation), and has a coordinate (x', y', z') in the new coordinate system (representing the position and orientation of the object after rotation), and then the coordinate rotation is shown as Fig. 4.

A relationship between the two coordinate values is established as: $(x, y, z, 1)^T = Rot(k, \theta)(x', y', z', 1)^T$, and the forth element '1' is added for the calculation uniformity of matrix operation. If there is a coordinate system rotates around axis X with an degree α, a point p has coordinate value (x, y, z) in the original coordinate system, and a coordinate (x', y', z') in the new coordinate system, then the following two equations hold.

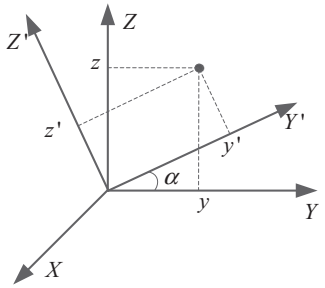

Fig. 4. Illustration of rotation matrix.

$$y = y'\cos\alpha - z'\sin\alpha, \quad z = y'\sin\alpha + z'\cos\alpha \tag{2}$$

Written in matrix form, Eq. (2) turns into

$$\begin{bmatrix} x \\ y \\ z \\ 1 \end{bmatrix} = \begin{bmatrix} 1 & 0 & 0 & 0 \\ 0 & \cos\alpha & -\sin\alpha & 0 \\ 0 & \sin\alpha & \cos\alpha & 0 \\ 0 & 0 & 0 & 1 \end{bmatrix} \begin{bmatrix} x' \\ y' \\ z' \\ 1 \end{bmatrix} \tag{3}$$

$$\text{Noted as}: \quad [M] = Rot(X, \alpha)[M'] \tag{4}$$

3.1.2. Translation matrix

Note $Trans(x, y, z)$ as the translation matrix for the operation of translating an object with an offset (t_x, t_y, t_z) along the axes $X \setminus Y \setminus Z$. A point p has coordinate value (x, y, z) in the original coordinate system, and a coordinate (x', y', z') in the new coordinate system, Then a relationship between the two coordinate values are established as: $(x, y, z, 1)^T = Trans(t_x, t_y, t_z)(x', y', z', 1)^T$, the forth element '1' is added for the calculation uniformity of matrix operation. It is easy to know that the translation matrix takes the form as:

$$Trans(t_x, t_y, t_z) = \begin{bmatrix} 1 & 0 & 0 & t_x \\ 0 & 1 & 0 & t_y \\ 0 & 0 & 1 & t_z \\ 0 & 0 & 0 & 1 \end{bmatrix} \tag{5}$$

3.2. Transformation matrix

The movement of an object involves translation and rotation of that object, and the corresponding transformation matrix for the movement of an object can be represented through the translation and rotation matrix. Note H_i^R as the transformation matrix for the operation of moving an object. A point p has coordinate value (x, y, z) in the original coordinate system, and a coordinate (x', y', z') in the new coordinate system, Then a relationship between the two coordinate values are: $(x, y, z, 1)^T = H_i^R(x', y', z', 1)^T$.

The movement of a rigid object can be decomposed into a sequence of rotation and movement. For instance, first rotate around X for a degree α, round Y for β and Z for γ, and then translate with an offset (t_x, t_y, t_z). The corresponding transformation matrix is formulated as:

$$H_i^R = Trans(t_x, t_y, t_z) \cdot Rot(z, \gamma) \cdot Rot(y, \beta) \cdot Rot(x, \alpha) \tag{6}$$

where $Rot(x, \alpha)$ and $Trans(t_x, t_y, t_z)$ are listed in Eqs. (4) and (5), $Rot(y, \beta)$, $Rot(z, \gamma)$ and H_i^R are:

$$Rot(y,\beta) = \begin{bmatrix} \cos\beta & 0 & \sin\beta & 0 \\ 0 & 1 & 0 & 0 \\ -\sin\beta & 0 & \cos\beta & 0 \\ 0 & 0 & 0 & 1 \end{bmatrix}, Rot(z,\gamma) = \begin{bmatrix} \cos\gamma & -\sin\gamma & 0 & 0 \\ \sin\gamma & \cos\gamma & 0 & 0 \\ 0 & 0 & 1 & 0 \\ 0 & 0 & 0 & 1 \end{bmatrix} \tag{7}$$

$$H_i^R = \begin{bmatrix} \cos\beta\cos\gamma & \sin\alpha\sin\beta\cos\gamma - \cos\alpha\sin\gamma & \cos\alpha\sin\beta\cos\gamma + \sin\alpha\sin\gamma & t_x \\ \cos\beta\sin\gamma & \sin\alpha\sin\beta\sin\gamma + \cos\alpha\cos\gamma & \cos\alpha\sin\beta\sin\gamma - \sin\alpha\cos\gamma & t_y \\ -\sin\beta & \sin\alpha\cos\beta & \cos\alpha\cos\beta & t_z \\ 0 & 0 & 0 & 1 \end{bmatrix} \tag{8}$$

3.3. Variation coupling

A new set of calculation principle is developed to analyze the relationship between different sources of variation and their coupling effect in this subsection. The homogenous transformation matrix (HTM) for the coordinate system transformation is used to represent the coordinate system transform. Note H_i^R as the HTM from the actual position and orientation of the ith characteristic, ${}^0H_i^R$ as the HTM from the nominal position and orientation of the ith characteristic, and the adjustment of the HTM is noted as δH_i^R. The HTM between the RCS and actual LCS_i is regarded as a two step transformation: (i). from the actual LCS_i to ${}^0LCS_i$, and (ii). from ${}^0LCS_i$ to RCS:

$$H_i^R = {}^0H_i^R \cdot \delta H_i^R \tag{9}$$

where $\delta H_i^R = \begin{bmatrix} 1 & -\theta_{iz}^R & \theta_{iy}^R & d_{ix}^R \\ \theta_{iz}^R & 1 & -\theta_{ix}^B & d_{iy}^R \\ -\theta_{iy}^R & \theta_{ix}^R & 1 & d_{iz}^R \\ 0 & 0 & 0 & 1 \end{bmatrix} = I_{4\times4} + \Delta_i^R$, $\Delta_i^R = \begin{bmatrix} 0 & -\theta_{iz}^R & \theta_{iy}^R & d_{ix}^R \\ \theta_{iz}^R & 0 & -\theta_{ix}^B & d_{iy}^R \\ -\theta_{iy}^R & \theta_{ix}^R & 0 & d_{iz}^R \\ 0 & 0 & 0 & 0 \end{bmatrix}$ is the differential transformation matrix (DTM) associating to the DMV x_i^R, $x_i^R = \begin{bmatrix} \left(d_i^R\right)^T & \left(\theta_i^R\right)^T \end{bmatrix}^T$.

Define the function $f(x_i^R) \rightarrow \Delta_i^R$ as the relationship between the elements of the DMV and the DTM. Thus:

$$H_i^R = {}^0H_i^R \cdot \delta H_i^R = {}^0H_i^R \cdot \left(I_{4\times4} + \Delta_i^R\right) = {}^0H_i^R + {}^0H_i^R \cdot \Delta_i^R \tag{10}$$

Assume there are two characteristics on the rotary workpiece, noted as LCS_i, $i = 1, 2$, and the HTM from LCS_1 to RCS, and form LCS_2 to LCS_1 are known, then

$$H_1^R = {}^0H_1^R + {}^0H_1^R \cdot \Delta_1^R, \text{and } H_2^1 = {}^0H_2^1 + {}^0H_2^1 \cdot \Delta_2^1 \tag{11}$$

and,

$$H_2^R = H_1^R \cdot H_2^1 = \left({}^0H_1^R + {}^0H_1^R \cdot \Delta_1^R\right) \cdot \left({}^0H_2^1 + {}^0H_2^1 \cdot \Delta_2^1\right) \tag{12}$$

Extend H_2^R, and neglect the second-order small values, and Eq. (13) can be obtained.

$$H_2^R = {}^0H_2^R\left(I + \left({}^0H_2^1\right)^{-1} \cdot \Delta_1^R \cdot {}^0H_2^1 + \Delta_2^1\right) \tag{13}$$

Since

$$H_2^R = {}^0H_2^R\left(I + \Delta_2^R\right) \tag{14}$$

Combining Eqs. (13) and (14),

$$\Delta_2^R = \left({}^0H_2^1\right)^{-1} \cdot \Delta_1^R \cdot {}^0H_2^1 + \Delta_2^1 \tag{15}$$

According to the work of Craig (2004), $\left({}^0H_2^1\right)^{-1} \cdot \Delta_1^R \cdot {}^0H_2^1 = {}^T\Delta_1^R$, where ${}^T\Delta_1^R = f\left(\begin{bmatrix} \left({}^0R_2^1\right)^T & -\left({}^0R_2^1\right)^T \cdot {}^0\hat{t}_2^1 \\ \mathbf{0} & \left({}^0R_2^1\right)^T \end{bmatrix} x_1^R\right)$, that is $\Delta_2^R = {}^T\Delta_1^R + \Delta_2^1$.

$\Delta_2^R = {}^T\Delta_1^R + \Delta_2^1$ is written as:

$$f(x_2^R) = f\left(\begin{bmatrix} \left({}^0R_2^1\right)^T & -\left({}^0R_2^1\right)^T \cdot {}^0\hat{t}_2^1 \\ \mathbf{0} & \left({}^0R_2^1\right)^T \end{bmatrix} x_1^R\right) + f(x_2^1) \tag{16}$$

Thus, according to the one-by-one mapping, Eq. (16) is rewritten as:

$$x_2^R = Q_2^1 x_1^R + x_2^1 \tag{17}$$

where $Q_2^1 = \begin{bmatrix} \left({}^0R_2^1\right)^T & -\left({}^0R_2^1\right)^T \cdot {}^0\hat{t}_2^1 \\ \mathbf{0} & \left({}^0R_2^1\right)^T \end{bmatrix}$.

It is easy to know that the ${}^0FCS$ and MCS are positional and orientational fixed to each other, thus there is a nominal HTM between the two coordinate systems, and ${}^0FCS$ is used to replace MCS to simplify the computation for this fixed relationship. The

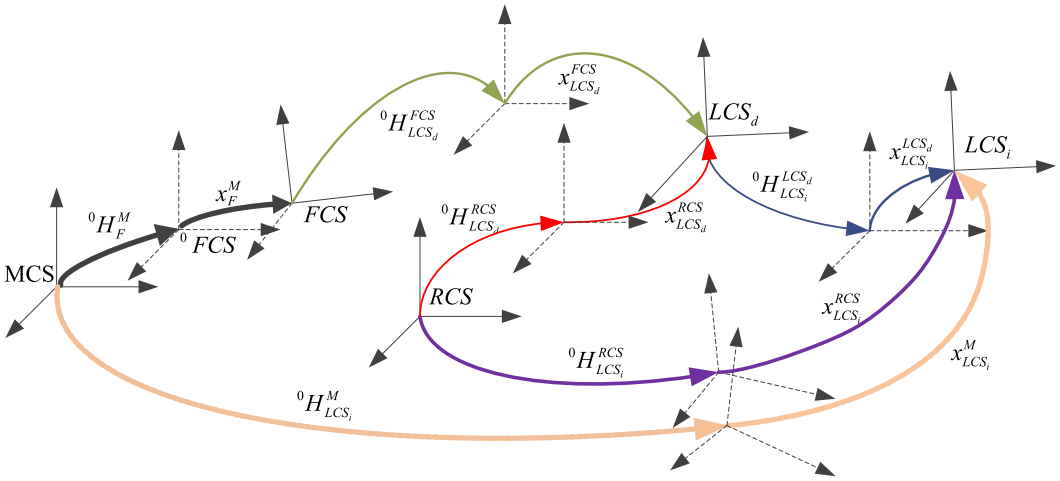

Fig. 5. Differential motion representation of variation accumulation of rotary workpiece.

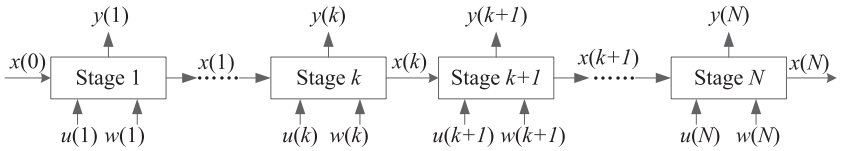

Fig. 6. Variation propagation of MTP.

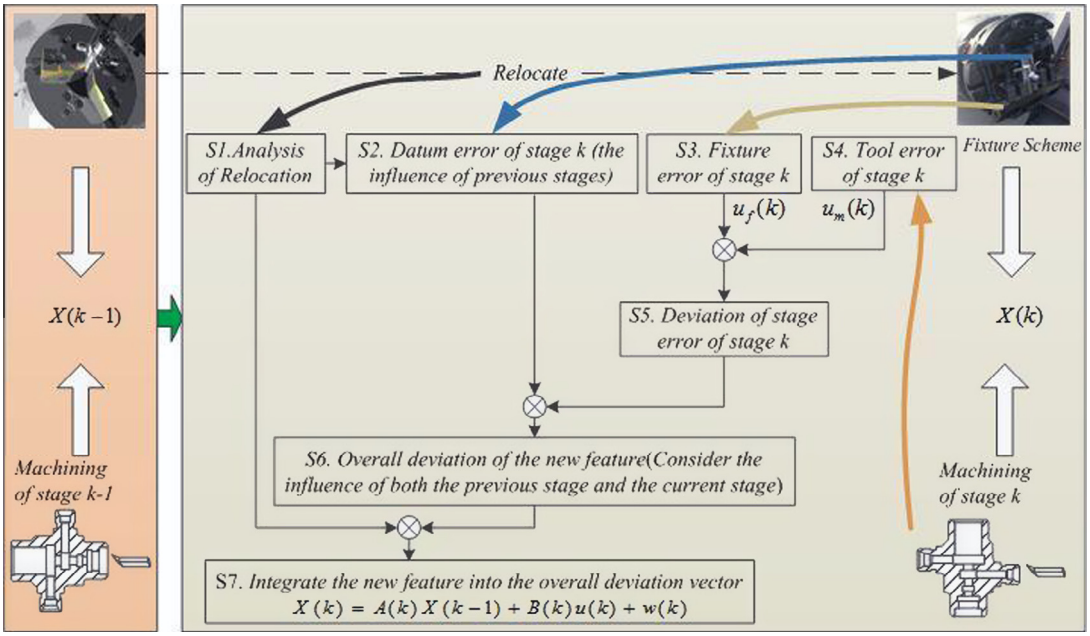

Fig. 7. Dimensional error computation procedure.

fixture imperfection leads to the misalignment between ^{0}FCS and FCS, noted as $x_{FCS}^{{}^0FCS}$.

If the flawed characteristics machined at previous stages are used as the datum characteristic, then the misalignment between the datum characteristic and the fixture (datum error) is introduced to the process, noted as x_{FCS}^{RCS}, shorted as $x_F^{R(k)}$ at stage k.

Since the characteristic machined are directly formed by the tool path, which is often programmed according to ^{0}FCS. The imperfection of the machined characteristic at current stage is illustrated by the actual path, thus the tool error is viewed as the deviation of the actual tool path from its programmed path, noted as $x_{i(k)}^{{}^0F}$, where $i(k)$ is the ith characteristic machined at stage k.

The characteristic error is also affected by the flawed fixture setup, thus the characteristic error contributed by the current stage is a mixed effect of tool error and fixture error. According to Eq. (17), the characteristic error contributed by the current stage is:

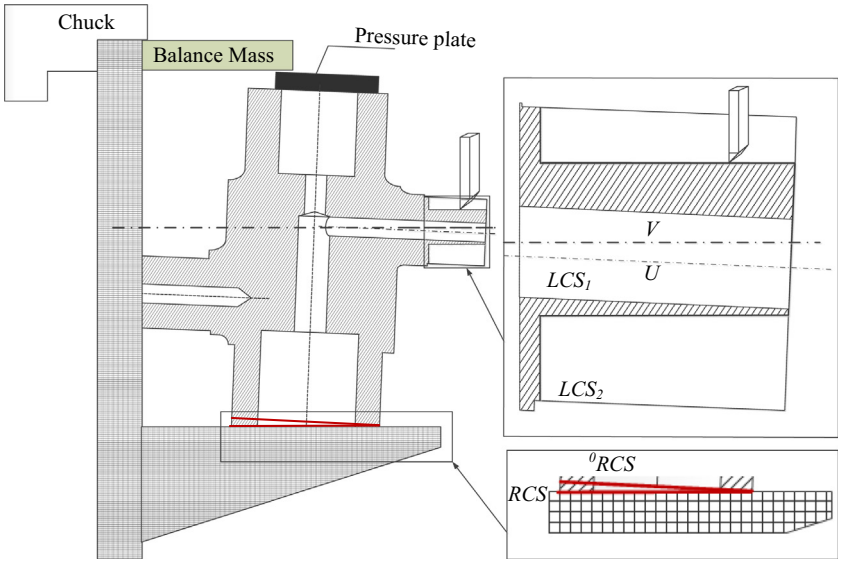

Fig. 8. Effects illustration of Datum error in rotary workpieces turning process.

$$x_{i(k)}^{F(k)} = Q_{i(k)}^{{}^0F(k)} \cdot x_{{}^0F(k)}^{F(k)} + x_{i(k)}^{{}^0F(k)} \tag{18}$$

Since the sources for the characteristic error can be generally classified into two categories: one from the current stage, and the other from the upstages (the flawed datum), the characteristic error is also contributed by the datum error $x_F^{R(k)}$. The mixed effects of the two sources is depicted by Eq. (17),

$$x_{i(k)}^{R(k)} = Q_{i(k)}^{F(k)} x_F^{R(k)} + x_{i(k)}^{F(k)} \tag{19}$$

The aforementioned relationships between different coordinate systems and the corresponding DMVs can be summarized by Fig. 5. The basic logic of Fig. 5 is that each kind of error can be represented by a nominal HTM and a DMV (with the same color). Take the fixture error for example. It is the deviation of MCS w.r.t. FCS as depicted in Fig. 2, which can be analyzed by further decomposing into two steps: (1) the nominal HTM from MCS to ^{0}FCS, and (2) the corresponding DMV x_F^M (Note that x_F^M and $x_F^{{}^0\mathrm{FCS}}$ are interchangeable through the nominal HTM from MCS to ^{0}FCS. We used the notation x_F^M instead of $x_F^{{}^0\mathrm{FCS}}$ here for two reasons. One is to help to keep the consistency of the paper. The DMVs are evaluated in the real coordinate system instead of the nominal coordinate system. The other reason is that it helps to differentiate the DMVs based on different coordinate system, such as $x_{\mathrm{LCS}_d}^{\mathrm{FCS}}$ and $x_{\mathrm{LCS}_d}^{\mathrm{RCS}}$ in Fig. 5. Both of the two steps are noted with bold black lines. Another example is also give for illustrating the tool error, which is noted with the light pink lines at the bottom of Fig. 5. The tool error can be deduced through (1) the HTM from MCS to $^0\mathrm{LCS}_i$, and (2) from $^0\mathrm{LCS}_i$ to $^0\mathrm{LCS}_i$ $\left(\text{which is the DMV } x_{\mathrm{LCS}_i}^M\right)$.

4. Derivation of the state space model for MTPs

4.1. Framework

There are two major types of variations at stage k for MTP with N stages (see Fig. 6): (i) the variations induced by previous stages through the flawed datum characteristics; (ii) the variations induced by current stage, including fixture error, tool error, etc.

The stage-wise variation accumulation property leads to the adoption of state space model, and the variation accumulation for MTP is represented:

$$\begin{aligned}\mathbf{x}(k) &= \mathbf{A}(k)\mathbf{x}(k-1) + \mathbf{B}(k)\mathbf{u}(k) + \mathbf{v}(k)\\ \mathbf{y}(k) &= \mathbf{C}(k)\mathbf{x}(k) + \mathbf{w}(k)\end{aligned} \tag{20}$$

where k is the stage index, $\mathbf{x}(k)$ is the product variation and $\mathbf{y}(k)$ is the corresponding measurement with respect to $\mathbf{x}(k)$, $\mathbf{u}(k)$ is the error caused by local stage, which contains two parts: the tool error and the fixture error in this paper, $\mathbf{A}(k)$ is the dynamic matrix representing the re-locate at the local stage, $\mathbf{B}(k)$ is the variation transformation matrix introduced by the local operation, $\mathbf{C}(k)$ is the observation matrix, and $\mathbf{v}(k)$ and $\mathbf{w}(k)$ are the model noises.

The whole computing procedure is illustrated in Fig. 7. From the beginning of each stage in MTPs, the rotary workpiece is relocated from stage $k-1$ and then fixed at stage k, introducing the change of RCS from $R(k-1)$ to $R(k)$ (see S1). Generally, the error raised from the fixturing process consists of two parts: (i) the datum error resulted from the locating datum (see S2), which is contributed by previous stages; (ii) the fixture error from the flawed fixture and worn locator (see S3). Since the turning process is performed on the flawed fixturing and positioning condition, the variation is affected by two type of errors (see S4 and S5). The variation of the workpiece characteristic is a comprehensive result of the previous stages and stage k (see S6). Finally, the state space model is built (S7).

4.2. Derivation of model

4.2.1. S1: Relocation error analysis

When a workpiece moves from stage $k-1$ to stage k, the RCS is also changed from $R(k-1)$ to $R(k)$, and the variation of characteristics is also changed due to RCS change. If the HTM from $R(k)$ to each FCS is known, then according to Eq. (17), the DMV of a characteristic's variation under coordinate system $R(k)$ is:

$$x_i^{R(k)} = x_i^{R(k-1)} - Q_i^{R(k)} \cdot x_R^{R(k-1)} \tag{21}$$

Note $\mathbf{x}_1(k)$ as the state vector representing the variation of all characteristics; it is a stack of the DMV, $x_i^{R(k)}$ of each characteristic at the beginning of stage k. Also note $\mathbf{x}(k-1)$ as a stack of $x_i^{R(k-1)}$ after all the operations at stage $k-1$. If there are M characteristics needs to be machined, then,

$$\mathbf{x}_1(k) = \mathbf{A}_1(k)\mathbf{x}(k-1) \tag{22}$$

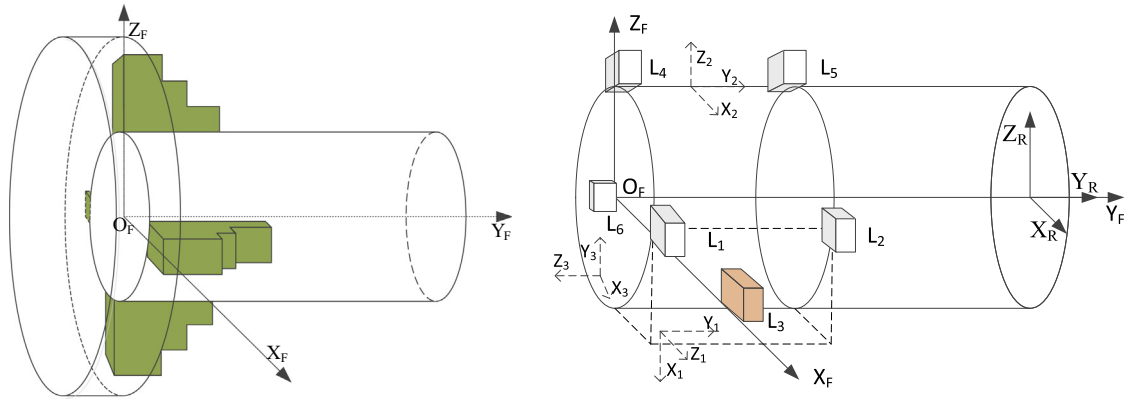

(a) Fixturing Scheme (b) Locator Analysis

Fig. 9. Illustration of 4-jaws chuck fixturing scheme in MTP.

$$\text{where } \mathbf{x}_1(k) = \begin{bmatrix} x_1^{R(k)} \\ \vdots \\ x_i^{R(k)} \\ \vdots \\ x_R^{R(k)} \\ \vdots \\ x_M^{R(k)} \end{bmatrix}, \mathbf{A}_1(k) = \begin{bmatrix} \mathbf{I} & \cdots & 0 & \cdots & 0 & \cdots & 0 \\ \vdots & \vdots & \vdots & \vdots & \vdots & \vdots & \vdots \\ 0 & \cdots & \mathbf{I} & \cdots & -\mathbf{Q}_i^{R(k)} & \cdots & 0 \\ \vdots & \vdots & \vdots & \vdots & \vdots & \vdots & \vdots \\ 0 & \cdots & 0 & \cdots & 0 & \cdots & 0 \\ \vdots & \vdots & \vdots & \vdots & \vdots & \vdots & \vdots \\ 0 & \cdots & 0 & \cdots & 0 & \cdots & \mathbf{I} \end{bmatrix},$$

$$\mathbf{x}(k-1) = \begin{bmatrix} x_1^{R(k-1)} \\ \vdots \\ x_i^{R(k-1)} \\ \vdots \\ x_r^{R(k-1)} \\ \vdots \\ x_M^{R(k-1)} \end{bmatrix}.$$

If the RCS is not changed when relocating a workpiece from stage k - 1 to stage k, then $\mathbf{x}_1(k) = \mathbf{x}(k-1)$.

4.2.2. S2: Datum error analysis

Datum error is caused by the flawed datum characteristic processed by previous stages, resulting in the deviation of the RCS with respect to FCS. For example, coaxiality variation is incurred in the presence of datum error in turning process (see Fig. 8). There is a datum error: the upper line is the nominal position of the datum characteristic, while the lower line is the actual datum characteristic position.

This paper analyzes the datum error in the four-jaw chuck fixturing scheme, one major fixturing strategy in turning process. As shown in Fig. 9(a), a 4-jaws chuck clamping has a FCS with Z axis perpendicular to the turning axis, Y axis along with the turning axis; and the X axis is perpendicular to the plane of $Y_F O_F Z_F$. Fig. 9(b) shows that the jaws limit the movement along $X \setminus Z$-axis, and the rotation round $X \setminus Z$-axis; the end of the jaw limits the movements along the Y-axis; with enough clamping force, the rotation round Y-axis is also limited. Under such condition a virtual locator is placed on the tangent plane where locator L_1 and L_2, the plane constrains the rotational motion round Y-axis. Thus locators $L_1 \sim L_6$ constrain all six degree of freedom of the workpiece.

The plane consisting of locator $L_1 \sim L_3$ is the primary datum plane (noted as $O_1X_1Y_1Z_1$,), which constrains one translational motion and two rotational motion. The secondary datum characteristic plane is the tangential plane locator L_4 and L_5 are placed (noted as $O_2X_2Y_2Z_2$), and the tertiary datum plane is the end plane containing locator L_6 (noted as $O_3X_3Y_3Z_3$).

The datum error induced by the flawed datum at stage k is seen as the discrepancy between the $R(k)$ and FCS(k), noted as $x_{FCS(k)}^{R(k)}$. The primary datum deviation with respect to $R(k)$ is noted as $x_1^{R(k)}$, and the second datum deviation with respect to $R(k)$ is noted as $x_2^{R(k)}$, the tertiary datum deviation with respect to $R(k)$ is noted as $x_3^{R(k)}$. Accordingly, $x_{FCS(k)}^{R(k)}$ is expressed in the linear combination of $x_1^{R(k)}$, $x_2^{R(k)}$ and $x_3^{R(k)}$. Let $T_1(k)$, $T_2(k)$ and $T_3(k)$ be the coefficient matrices, and $x_{FCS(k)}^{R(k)}$ is expressed as:

$$x_{FCS(k)}^{R(k)} = T_1(k)x_1^{R(k)} + T_2(k)x_2^{R(k)} + T_3(k)x_3^{R(k)} \tag{23}$$

$p_1 \sim p_6$ are the points on the workpiece that directly touching the six locators, $L_1 \sim L_6$, on the fixture, with coordinate value $p_1^F \sim p_6^F$ with respect to FCS respectively. Under the direct touching condition, the Z value of each locator is zero. That is:

$$\begin{cases} \left[H_R^1 \cdot H_F^R \cdot \tilde{p}_1^F\right]_3 = 0 \\ \left[H_R^1 \cdot H_F^R \cdot \tilde{p}_2^F\right]_3 = 0 \\ \left[H_R^1 \cdot H_F^R \cdot \tilde{p}_3^F\right]_3 = 0 \\ \left[H_R^2 \cdot H_F^R \cdot \tilde{p}_4^F\right]_3 = 0 \\ \left[H_R^2 \cdot H_F^R \cdot \tilde{p}_5^F\right]_3 = 0 \\ \left[H_R^3 \cdot H_F^R \cdot \tilde{p}_6^F\right]_3 = 0 \end{cases} \tag{24}$$

Take p_1 for example, given that $H_R^1 = (\bar{\Delta}_1^R + I) \cdot {}^0H_R^1$ and $H_F^R = {}^0H_F^R \cdot (\Delta_F^R + I)$ (Paul, 1981)

$$\left[\left(\bar{\Delta}_1^R \cdot {}^0H_F^1 + {}^0H_F^1 \cdot \Delta_F^R + {}^0H_F^1\right) \cdot \tilde{p}_1^F\right]_3 = 0 \tag{25}$$

Under nominal fixture locating condition, $[{}^0H_F^1 \cdot \tilde{p}_1^F]_3 = 0$, Eq. (25) is rewritten as:

$$\left[\Delta_1^R \cdot {}^0H_F^1 \cdot \tilde{p}_1^F\right]_3 = \left[{}^0H_F^1 \cdot \Delta_F^R \cdot \tilde{p}_1^F\right]_3 \tag{26}$$

Note $\Delta_1^R = \begin{bmatrix} \hat{\theta}_2^R & d_2^R \\ 0 & 1 \end{bmatrix}, {}^0H_F^1 = \begin{bmatrix} {}^0n_F^1 & {}^0o_F^1 & {}^0a_F^1 & {}^0t_F^1 \\ 0 & 0 & 0 & 1 \end{bmatrix}$, then the two sides of Eq. (25) is converted to:

$$\left[\Delta_1^R \cdot {}^0H_F^1 \cdot \tilde{p}_1^F\right]_3 = \left[\left[\theta_1^R \times {}^0n_F^1\right]_3 \left[\theta_1^R \times {}^0o_F^1\right]_3 \left[\theta_1^R \times {}^0a_F^1\right]_3 \left[\theta_1^R \times {}^0t_F^1 + d_1^R\right]_3\right] \cdot \tilde{p}_1^F$$

$$\left[{}^0H_F^1 \cdot \Delta_F^R \cdot \tilde{p}_1^F\right]_3 = \begin{bmatrix} \left[{}^0a_1^F\right]^T & \left[p_1^F \times {}^0a_1^F\right]^T \end{bmatrix} \cdot x_F^R$$

Thus,

$$\begin{bmatrix} \left[{}^0a_1^F\right]^T & \left[p_1^F \times {}^0a_1^F\right]^T \end{bmatrix} \cdot x_F^R = \left[\left[\theta_1^R \times {}^0n_F^1\right]_3 \quad \left[\theta_1^R \times {}^0o_F^1\right]_3 \left[\theta_1^R \times {}^0a_F^1\right]_3 \left[\theta_1^R \times {}^0t_F^1 + d_1^R\right]_3\right] \cdot \tilde{p}_1^F \tag{27}$$

By applying the same procedure from Eqs. (25)–(27), the latter five equations in equation set (24) for the touching condition of $p_2 \sim p_6$ can be obtained,

$$\begin{bmatrix} [{}^0a_1^F]^T & [p_1^F \times {}^0a_1^F]^T \\ [{}^0a_1^F]^T & [p_2^F \times {}^0a_1^F]^T \\ [{}^0a_1^F]^T & [p_3^F \times {}^0a_1^F]^T \\ [{}^0a_2^F]^T & [p_4^F \times {}^0a_2^F]^T \\ [{}^0a_2^F]^T & [p_5^F \times {}^0a_2^F]^T \\ [{}^0a_3^F]^T & [p_6^F \times {}^0a_3^F]^T \end{bmatrix} x_F^R = \begin{bmatrix} \left[[\theta_1^R \times {}^0n_F^1]_3 \quad [\theta_1^R \times {}^0o_F^1]_3 \quad [\theta_1^R \times {}^0a_F^1]_3 \quad \left[\theta_1^R \times {}^0t_F^1 + d_1^R\right]_3\right] \cdot \tilde{p}_1^F \\ \left[[\theta_1^R \times {}^0n_F^1]_3 \quad [\theta_1^R \times {}^0o_F^1]_3 \quad [\theta_1^R \times {}^0a_F^1]_3 \quad \left[\theta_1^R \times {}^0t_F^1 + d_1^R\right]_3\right] \cdot \tilde{p}_2^F \\ \left[[\theta_1^R \times {}^0n_F^1]_3 \quad [\theta_1^R \times {}^0o_F^1]_3 \quad [\theta_1^R \times {}^0a_F^1]_3 \quad \left[\theta_1^R \times {}^0t_F^1 + d_1^R\right]_3\right] \cdot \tilde{p}_3^F \\ \left[[\theta_2^R \times {}^0n_F^2]_3 \quad [\theta_2^R \times {}^0o_F^2]_3 \quad [\theta_2^R \times {}^0a_F^2]_3 \quad \left[\theta_2^R \times {}^0t_F^2 + d_2^R\right]_3\right] \cdot \tilde{p}_4^F \\ \left[[\theta_2^R \times {}^0n_F^2]_3 \quad [\theta_2^R \times {}^0o_F^2]_3 \quad [\theta_2^R \times {}^0a_F^2]_3 \quad \left[\theta_2^R \times {}^0t_F^2 + d_2^R\right]_3\right] \cdot \tilde{p}_5^F \\ \left[[\theta_3^R \times {}^0n_F^3]_3 \quad [\theta_3^R \times {}^0o_F^2]_3 \quad [\theta_3^R \times {}^0a_F^3]_3 \quad \left[\theta_3^R \times {}^0t_F^3 + d_3^R\right]_3\right] \cdot \tilde{p}_6^F \end{bmatrix} \tag{28}$$

The computation of Eq. (28) is simplified by the orthogonality of $O_1X_1Y_1Z_1$, $O_2X_2Y_2Z_2$ and $O_3X_3Y_3Z_3$. Given the nominal position of the three datum characteristics and the position of the six locators with respect to FCS as:

$$p_1^F = \begin{bmatrix} r & p_{1y}^F & p_{1z}^F \end{bmatrix}^T, p_2^F = \begin{bmatrix} r & p_{2y}^F & p_{2z}^F \end{bmatrix}^T, p_3^F = \begin{bmatrix} r & p_{3y}^F & p_{3z}^F \end{bmatrix}^T,$$

$$p_4^F = \begin{bmatrix} p_{4x}^F & p_{4y}^F & r \end{bmatrix}^T, p_5^F = \begin{bmatrix} p_{5x}^F & p_{5y}^F & r \end{bmatrix}^T, p_6^F = \begin{bmatrix} p_{6x}^F & 0 & p_{6z}^F \end{bmatrix}^T.$$

$${}^0H_F^1 = \begin{bmatrix} 0 & 0 & -1 & r \\ 0 & 1 & 0 & {}^0t_{Fy}^1 \\ 1 & 0 & 0 & 0 \\ 0 & 0 & 0 & 1 \end{bmatrix} {}^0H_F^2 = \begin{bmatrix} 1 & 0 & 0 & 0 \\ 0 & 1 & 0 & {}^0t_{Fy}^2 \\ 0 & 0 & 1 & r \\ 0 & 0 & 0 & 1 \end{bmatrix}$$

$${}^0H_F^3 = \begin{bmatrix} 1 & 0 & 0 & {}^0t_{Fx}^3 \\ 0 & 0 & 1 & {}^0t_{Fy}^3 \\ 0 & -1 & 0 & 0 \\ 0 & 0 & 0 & 1 \end{bmatrix}$$

where r is the radius of the rotary workpiece.

The equation set (28) is simplified to Eq. (29).

$$\begin{bmatrix} 1 & 0 & 0 & 0 & p_{1z}^F & -p_{1y}^F \\ 1 & 0 & 0 & 0 & p_{2z}^F & -p_{2y}^F \\ 1 & 0 & 0 & 0 & p_{3z}^F & p_{3y}^F \\ 0 & 0 & 1 & p_{4y}^F & -p_{4x}^F & 0 \\ 0 & 0 & 1 & p_{5y}^F & -p_{5x}^F & 0 \\ 0 & -1 & 0 & p_{6z}^F & 0 & -p_{6x}^F \end{bmatrix} \cdot \begin{bmatrix} d_{Fx}^R \\ d_{Fy}^R \\ d_{Fz}^R \\ \theta_{Fx}^R \\ \theta_{Fy}^R \\ \theta_{Fz}^R \end{bmatrix} = \begin{bmatrix} (p_{1y}^F + {}^0t_{Fy}^1) \cdot \theta_{1\alpha}^R + (p_{1z}^F - R_0) \cdot \theta_{1\beta}^R + d_{1z}^R \\ (p_{2y}^F + {}^0t_{Fy}^1) \cdot \theta_{1\alpha}^R + (p_{2z}^F - R_0) \cdot \theta_{1\beta}^R + d_{1z}^R \\ (p_{3y}^F + {}^0t_{Fy}^1) \cdot \theta_{1\alpha}^R + (p_{3z}^F - R_0) \cdot \theta_{1\beta}^R + d_{1z}^R \\ (p_{4y}^F + {}^0t_{Fy}^2) \cdot \theta_{2\alpha}^R - p_{4x}^F \cdot \theta_{2\beta}^R + d_{2z}^R \\ (p_{5y}^F + {}^0t_{Fy}^2) \cdot \theta_{2\alpha}^R - p_{5x}^F \cdot \theta_{2\beta}^R + d_{2z}^R \\ (p_{6z}^F + {}^0t_{Fy}^3) \cdot \theta_{3\alpha}^R - (p_{6x}^F + {}^0t_{Fx}^3) \cdot \theta_{3\beta}^R + d_{3z}^R \end{bmatrix} \tag{29}$$

There are six variables and six equations in equation set (29), thus the equation set (29) can be solved by arranging the result in the form of Eq. (23). Then T_1, T_2 and T_3 is obtained:

$$T_1 = \begin{bmatrix} 0 & 0 & 1 & {}^0t_{Fy}^1 & -r & 0 \\ 0 & 0 & 0 & -p_{6x}^F & \frac{-p_{6z}^F(p_{4x}^F - p_{5x}^F)}{p_{4y}^F - p_{5y}^F} & 0 \\ 0 & 0 & 0 & 0 & \frac{-\left(p_{4x}^F \cdot p_{5y}^F - p_{5x}^F \cdot p_{4y}^F\right)}{p_{4y}^F - p_{5y}^F} & 0 \\ 0 & 0 & 0 & 0 & \frac{p_{4x}^F - p_{5x}^F}{p_{4y}^F - p_{5y}^F} & 0 \\ 0 & 0 & 0 & 0 & 1 & 0 \\ 0 & 0 & 0 & -1 & 0 & 0 \end{bmatrix}, T_2 = \begin{bmatrix} 0 & 0 & 0 & 0 & 0 & 0 \\ 0 & 0 & 0 & -p_{6z}^F & \frac{-p_{6z}^F(p_{4x}^F - p_{5x}^F)}{p_{4y}^F - p_{5y}^F} & 0 \\ 0 & 0 & 0 & {}^0t_{Fy}^2 & \frac{p_{4x}^F \cdot p_{5y}^F - p_{5x}^F \cdot p_{4y}^F}{p_{4y}^F - p_{5y}^F} & 0 \\ 0 & 0 & 0 & 0 & \frac{-(p_{4x}^F - p_{5x}^F)}{p_{4y}^F - p_{5y}^F} & 0 \\ 0 & 0 & 0 & 0 & 0 & 0 \\ 0 & 0 & 0 & 0 & 0 & 0 \end{bmatrix},$$

$$T_3 = \begin{bmatrix} 0 & 0 & 0 & 0 & 0 & 0 \\ 0 & 0 & 1 & -p_{6z}^F - {}^0t_{Fy}^3 & p_{6x}^F + {}^0t_{Fx}^3 & 0 \\ 0 & 0 & 0 & 0 & 0 & 0 \\ 0 & 0 & 0 & 0 & 0 & 0 \\ 0 & 0 & 0 & 0 & 0 & 0 \\ 0 & 0 & 0 & 0 & 0 & 0 \end{bmatrix}$$

Hence, the datum error occurred at stage k is:

$$X_{FCS(k)}^{R(k)} = A_2(k)X_1(k) \tag{30}$$

where $A_2(k) = [0 \cdots T_1(k) \cdots T_2(k) \cdots T_3(k) \cdots 0]_{6\times 6M}$

4.2.3. S3: Fixture error analysis

Fixture error is the actual positional and orientational deviation of FCS with respect to ^{0}FCS. If fixture error exits in the machining process, the coaxiality error is also introduced. As shown in Fig. 10, once a flawed fixture error exists, the coaxiality error of the machined characteristic is thus incurred.

As shown in Fig. 9(b), a workpiece is located by six locators, $L_1 \sim L_6$. The error of $L_1 \sim L_6$ is represented by $u_f(k) = [\Delta L_{1z}, \Delta L_{2z}, \Delta L_{3z}, \Delta L_{4z}, \Delta L_{5z}, \Delta L_{6z}]^T$. The fixture error is obtained according to the work of Cai, Hu, and Yuan (1997):

$$x_{{}^0FCS(k)}^{FCS(k)} = A_3(k)u_f(k) = -T_4(k)u_f(k) \tag{31}$$

where $T_4 = \begin{bmatrix} 0 & 0 & 0 & 1 & 0 & 0 \\ \frac{L_{6x}}{L} & \frac{-L_{6x}}{L} & 0 & \frac{-L_{6z}}{L} & \frac{L_{6z}}{L} & 1 \\ 1 & 0 & 0 & 0 & 0 & 0 \\ \frac{1}{L} & \frac{-1}{L} & 0 & 0 & 0 & 0 \\ \frac{L_{3y}-L}{L \cdot L_{3z}} & \frac{-L_{3y}}{L \cdot L_{3z}} & \frac{1}{L_{3z}} & 0 & 0 & 0 \\ 0 & 0 & 0 & \frac{-1}{L} & \frac{1}{L} & 0 \end{bmatrix}$

4.2.4. S4: Turning tool error analysis

Since the tool path is programmed in ^{0}FCS, the tool error is also seen as the deviation of the actual cutting tool path from the programmed (nominal) tool path in ^{0}FCS. The tool error of one characteristic machined at stage k is:

$$x_{i(k)}^{{}^0FCS} = [\Delta x, \Delta y, \Delta z, \Delta\psi, \Delta\theta, \Delta\varphi] \tag{32}$$

In Fig. 11, the tool is programmed with a path $M_0 \to {}^0M_1$, however, the actual tool path is $M_0 \to M_1$, then the error has a angle α round X axis, forming an perpendicity error.

4.2.5. S5: Stage error analysis

If there are $l(k)$ newly generated characteristics at stage k, then according to Eq. (18), the stage error of stage k is

$$u_s(k) = A_4(k)x_{{}^0FCS_k}^{FCS_k} + u_t(k) \tag{33}$$

where $A_4(k) = \left[G_1(k)^T \cdots G_i(k)^T \cdots G_l(k)^T\right]^T$, $G_i(k) = \begin{bmatrix} \left({}^0R_{i(k)}^{{}^0FCS(k)}\right)^T & -\left({}^0R_{i(k)}^{{}^0FCS(k)}\right)^T \cdot \left({}^0t_{i(k)}^{{}^0FCS(k)}\right) \\ 0 & \left({}^0R_{i(k)}^{{}^0FCS(k)}\right)^T \end{bmatrix}$, $u_t(k)$ is a stack of $x_{i(k)}^{{}^0FCS}$, corresponding to tool errors for all characteristics machined at stage k, and $u_s(k)$ is the error contributed by current stage, which is a coupling error of fixture error and tool error, both $u_t(k)$ and $u_s(k)$ have a dimension of $6l(k)\times 1$, and $A_4(k)$ has a dimension of $6l(k)\times 6$.

4.2.6. S6: Variation of characteristics generated at stage K

The variation of the newly generated characteristic is represented by $X^{new}(k) = \left[\left(x_{1(k)}^{R(k)}\right)^T \cdots \left(x_{i(k)}^{R(k)}\right)^T \cdots \left(x_{l(k)}^{R(k)}\right)^T\right]^T$.

According to Eq. (19), it is calculated:

$$X^{new}(k) = A_5(k) \cdot x_{FCS(k)}^{R(k)} + u_s(k) \tag{34}$$

where $u_s(k)$ is the error induced by stage k, $x_{FCS(k)}^{R(k)}$ is datum error, $A_5(k) = [D_1(k)^T \cdots D_i(k)^T \cdots D_l(k)^T]^T$ is coefficient matrix, in which $D_i(k)^T = \begin{bmatrix} \left({}^0R_{i(k)}^{FCS_k}\right)^T & -\left({}^0R_{i(k)}^{FCS_k}\right)^T \cdot \left({}^0t_{i(k)}^{FCS_k}\right) \\ 0 & \left({}^0R_{i(k)}^{FCS_k}\right)^T \end{bmatrix}$.

4.2.7. S7: Deduction of state space model

By combining the variations of characteristics generated at stage k and variation of other characteristics at upstream stages, the state vector is obtained by coupling the variation of characteristics generated at upstream stages before stage k ($\mathbf{x}_1(k)$ in Eq. (22)) and the variation generated at stage k,

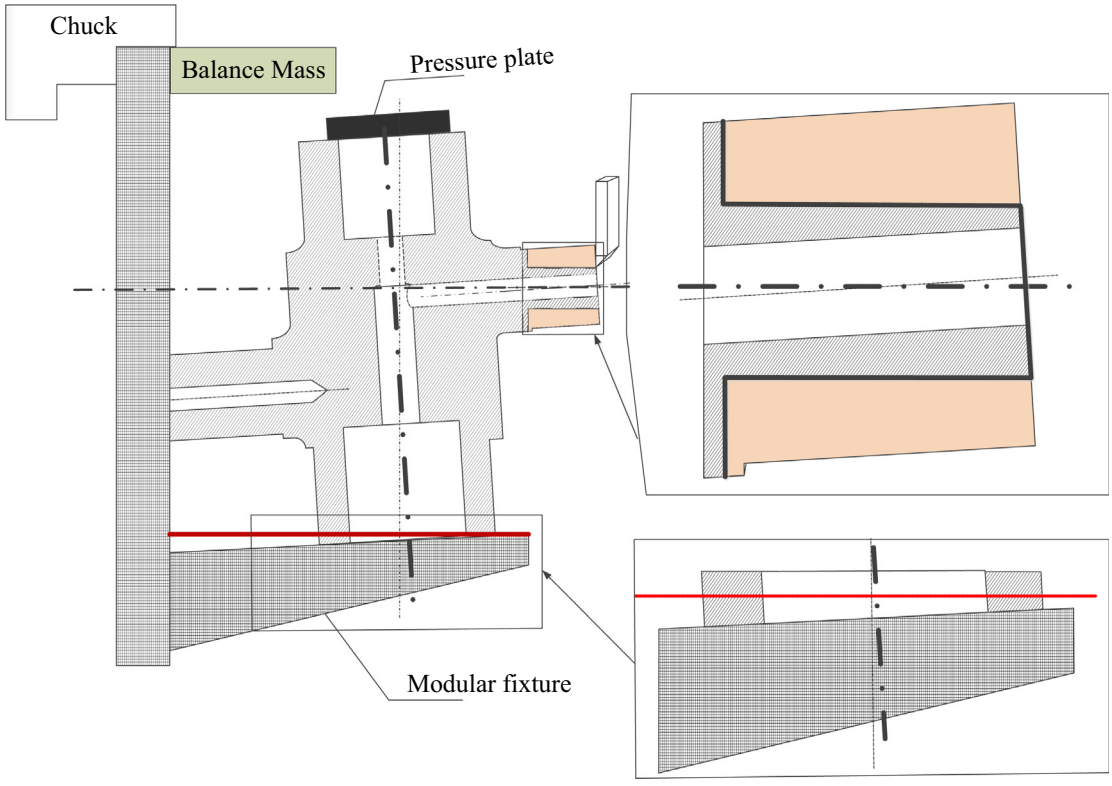

Fig. 10. Effects illustration of fixture error in rotary parts machining process.

$$x(k) = x_1(k) + A_6(k)x_{new}(k) \tag{35}$$

where $A_6(k)$ is a selective matrix with all the identity elements corresponding to the newly generated dimensional error at stage k (see Eq. (36)).

$$A_6(k) = \begin{bmatrix} 0 & \cdots & 0 & \cdots & 0 \\ \vdots & \vdots & \vdots & \vdots & \vdots \\ I_{6\times6} & \cdots & 0 & \cdots & 0 \\ \vdots & \vdots & \vdots & \vdots & \vdots \\ 0 & \cdots & I_{6\times6} & \cdots & 0 \\ \vdots & \vdots & \vdots & \vdots & \vdots \\ 0 & \cdots & 0 & \cdots & I_{6\times6} \\ \vdots & \vdots & \vdots & \vdots & \vdots \\ 0 & \cdots & 0 & \cdots & 0 \end{bmatrix} \tag{36}$$

By substituting Eqs. (30)–(34) into (35), the state space model for MTPs is obtained,

$$\begin{aligned} X(k) &= X_1(k) + A_6(k)X^{new}(k) \\ &= [A_1(k) + A_6(k)A_5(k)A_2(k)A_1(k)]X(k-1) \\ &+ A_6(k)[A_4(k)A_3(k) \;\; I_{6\times6}]\begin{bmatrix} u_f(k) \\ u_t(k) \end{bmatrix} = A(k)X(k-1) + B(k)u(k) \end{aligned} \tag{37}$$

So far, all of the coefficients of state space model (20) for MTP are obtained.

$$\begin{aligned} A(k) &= [A_1(k) + A_6(k)A_5(k)A_2(k)A_1(k)] \\ B(k) &= [A_6(k)A_4(k)A_3(k) \quad A_6(k)] \end{aligned} \tag{38}$$

The coefficient for the measurement can be deduced in the same way. In order to shorten the passage, it is not listed in this paper.

5. Case study

5.1. Experiment setup

The proposed state space model for MTPs is validated by one type of rotary workpieces, produced by a domestic machining corporation whose primal products are valve shells. Fig. 12(a) depicts a raw part of the valve shell; Fig. 12(b) is a 3-D model of the final product. Fig. 12(c) is a cross-section drawn of valve shell from the axles of end $A \setminus B \setminus C \setminus D$ after the MTP. Due to confidentiality requirements, the tolerance in the part drawn is deleted. Fig. 13 shows the real tuning process of the valve shell.

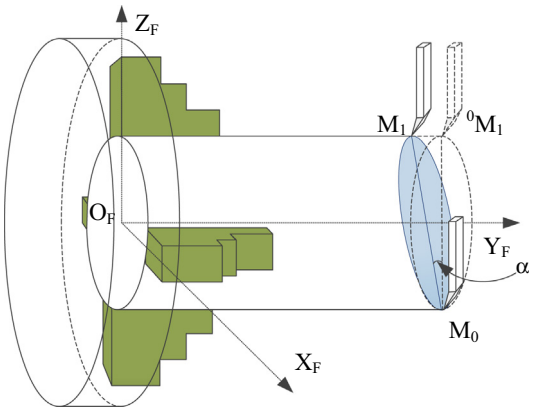

Fig. 11. Illustration of tool error.

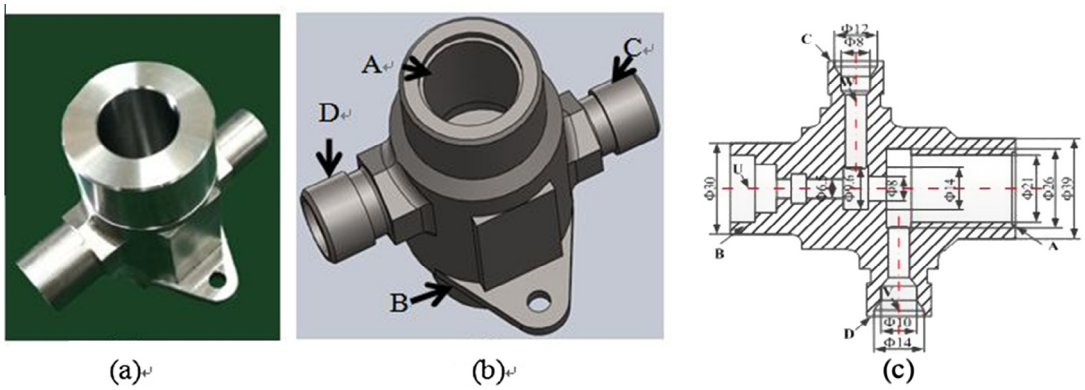

Fig. 12. Valve shell part model.

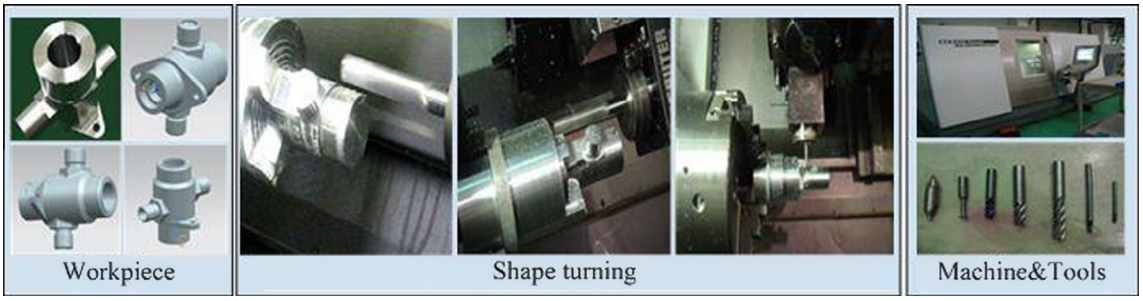

Fig. 13. Workpiece turning process.

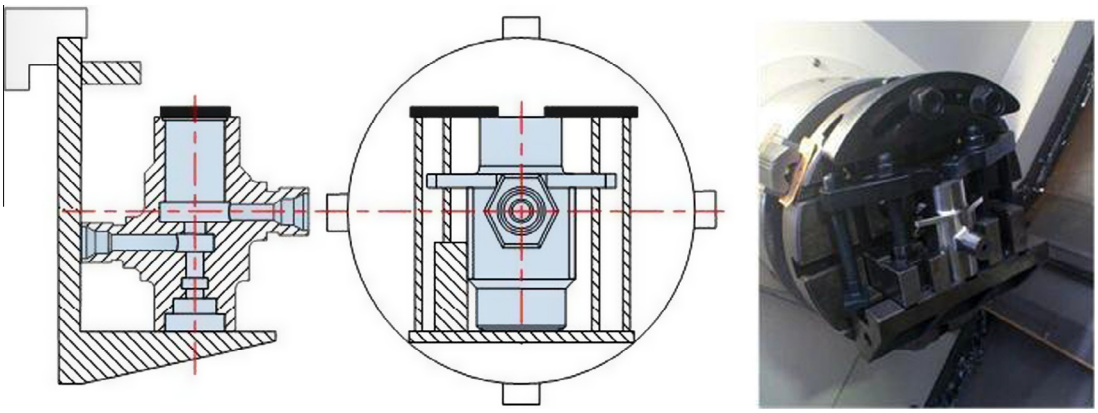

Fig. 14. Illustration of the first fixture scheme.

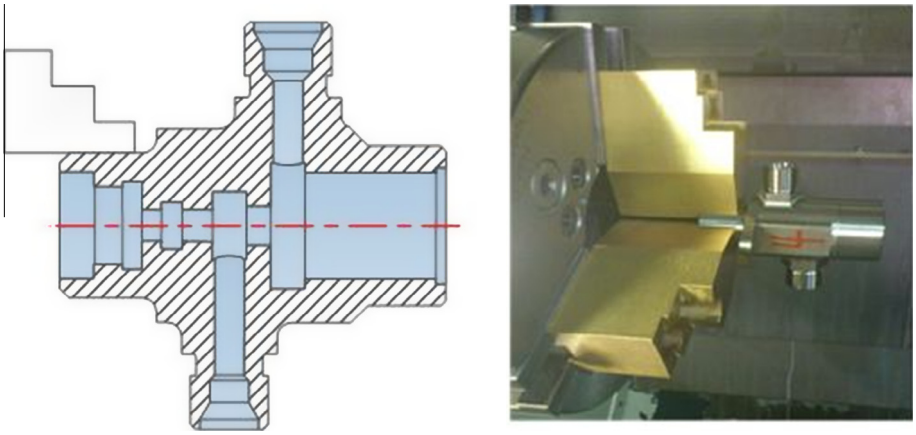

Fig. 15. Illustration of the second fixture scheme.

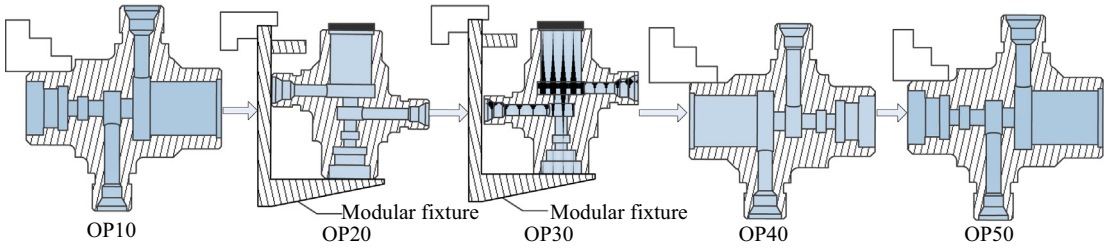

Fig. 16. Illustration of valve shell MTP.

Table 1
Nominal positions and orientations of KPCs.

No.	Fixture scheme	KPCs	Designed tolerances	Nominal position t_n^R/mm	Nominal angular ω_n^R/rad
OP10	B, 4-jaws Chuck	Hole Φ21	Coaxiality0.1|U|	[0,0,−29]	[0,0,0]
		ExcircleΦ39	Not a KPC	[0,0,0]	[0,0,0]
OP20	B downward, modular fixture (Process end D)	Hole Φ14	Cylindricity0.02|V|	[−42,0,−32.5]	[π/2,0,π/2]
		Hole Φ10	Cylindricity0.02|V|	[−32,0,−32.5]	[π/2,0,π/2]
OP30	B downward, modular fixture (Process end C)	Hole Φ12	Cylindricity0.02|W|	[−42,0,−44.5]	[−π/2,0,−π/2]
		Hole Φ8	Cylindricity0.02|W|	[−32,0,−32.5]	[−π/2,0,−π/2]
OP40	A, 4-jaws Chuck	Slot Φ9.6	Coaxiality0.05|U|	[0,0,−66.5]	[0,π,0]
		Hole Φ6.5	Coaxiality0.05|U|	[0,0,−62.5]	[0,π,0]
		ExcircleΦ30	Not a KPC	[0,0,−79.5]	[0,π,0]
OP50	B, 4-jaws Chuck	Slot Φ26	Depth 36 ± 0.1|A|	[0,0,−36]	[0,0,0]
		Slot Φ14	Depth48 ± 0.1|A|	[0,0,−48]	[0,0,0]
		Hole Φ8	Coaxialityjn0.05|U|	[0,0,−35.5]	[0,0,0]

Table 2
Predicted values of KPCs' variations.

KPCs	Designed tolerances	x	y	z	i	j	k
Hole Φ21	Coaxiality0.1|U|	0	−0.0193	0	0.0007	0	0
ExcircleΦ39	Not a KPC	0	−0.0387	0	0	0	0
Hole Φ14	Cylindricity0.02|V|	0.0120	0.0280	0	0	−0.0002	−0.0008
Hole Φ10	Cylindricity0.02|V|	0.0120	0.0213	0	0	−0.0002	−0.0008
Hole Φ12	Cylindricity0.02|W|	−0.0040	0.0280	0	0	−0.0002	−0.0008
Hole Φ8	Cylindricity0.02|W|	−0.0040	0.0213	0	0	−0.0002	−0.0008
Slot Φ9.6	Coaxiality0.05|U|	0	−0.0027	0	0.0013	0	0
Hole Φ6.5	Coaxiality0.05|U|	0	0.0017	0	0.0007	0	0
ExcircleΦ30	Not a KPC	0	−0.0193	0	0.0013	0	0
Slot Φ26	Depth 36 ± 0.1|A|	0	0	0	0.0007	0	0
Slot Φ14	Depth48 ± 0.1|A|	0	0	0	0.0007	0	0
Hole Φ8	Coaxiality ± 0.05|U|	0	0	0	0.0007	0	0

Table 3
Measurement values of KPCs' variations.

KPCs	Designed tolerances	x	y	z	i	j	k
Hole Φ21	Coaxiality0.1|U|	0	−0.020	0	0.001	0	0
ExcircleΦ39	Not a KPC	0	−0.040	0.001	0	0	0
Hole Φ14	Cylindricity0.02|V|	0.013	0.027	0	0	0	−0.001
Hole Φ10	Cylindricity0.02|V|	0.013	0.023	0	0	0	−0.001
Hole Φ12	Cylindricity0.02|W|	−0.004	0.027	0	0	0	−0.001
Hole Φ8	Cylindricity0.02|W|	−0.004	0.022	0.001	0	0	−0.001
Slot Φ9.6	Coaxiality0.05|U|	0	−0.002	0	0.001	0	0
Hole Φ6.5	Coaxiality0.05|U|	0	0.002	0	0.001	0	0
ExcircleΦ30	Not a KPC	0	−0.020	0.000	0.001	0	0
Slot Φ26	Depth 36 ± 0.1|A|	0	0	0.001	0.001	0	0
Slot Φ14	Depth48 ± 0.1|A|	0	0	0	0.001	0	0
Hole Φ8	Coaxiality ± 0.05|U|	0	0	0.001	0.001	0	0

The turning process is implemented using a computer numerical control (CNC) machining center (CTX420). The whole process is performed under two fixture schemes. One fixture scheme is shown as Fig. 14 and the other one is the chuck jaws scheme shown as Fig. 15. The turning process is mainly composed by five operations, noted as OP10–OP50 (see Fig. 16). The workpiece tolerance are given in Table 1.

End plane A and B are important datum characteristics whose errors are introduced as datum errors affecting the machining precision of other characteristics, such as the holes and slots. The excirlce machined at OP10 is the datum at OP40, thus the error of OP10 will be accumulated to the variation of characteristics machined at OP40. Similarly, the variation of characteristics machined at OP40 is one of the important sources of variation for OP50. The turning process of such a valve shell is a typical MTP where variations are propagated, transmitted and synthesized through all the stages.

6. Results and discussion

The model is programmed using MATLAB 2010®. For each stage, the variation of the workpiece characteristics can be output automatically once the fixture error and tool error are input to the program. The three-dimensional variation propagation model for rotary workpieces is used for KPC variation prediction. Table 2 is the predicted values of KPCs' variations with fixture error at each stage equals to $[0, 0.01, 0, 0, 0, 0]$.

The actual measurements for all these characteristics are listed in Table 3. Comparing Tables 2 and 3, the overall differences between the predicted values and the actual measurements are reasonably small. Take ∅8 for example, the coaxiality requirement is 0.02 mm with respect to axis *W*. The prediction error is 0.004 mm, which means a quite small deviation between the model prediction and the actual values. For other characteristics, the prediction error between the predicted value and the actual measurement also exist, and one main reason may be accounted to the tool error, which is set up as zero in the prediction model in the experiment. Whereas the actual tool error in the turning process are nonzero values. The small discrepancies between the predicted value and the actual measurement validate the proposed model.

In addition, the proposed model also shows the variation patterns. Take hole Φ14 and hole Φ10 from OP20 for examples, they are both machined at OP20 under the modular fixture scheme. They have a clear similar variation pattern since the fixture scheme and the tool cutting are the same; the difference is caused by the positional relationship with respect to the datum and some other factors, such as the thermal and the cutting force change.

9. Conclusions

Based on the definition of four types of coordinate systems and four types of errors, the paper conducts an analysis of fixture error, datum error and their coupling effect under jaws chuck fixturing scheme. A state space model of the three-dimensional variation propagation for MTP is built based on the analysis of turning procedure and the coupling analysis, depicting the transmission and accumulation of the variation of product characteristics among stages. A valve shell turning case is chosen to verify the proposed model, and the results show that the proposed model yield satisfactory predict precision. The proposed model can be further applied into tolerance allocation, process control, fault diagnosis and process improvement.

Acknowledgements

The authors greatly acknowledge the editor and the referees for their valuable comments and suggestions that have led to a substantial improvement of the paper. This work was supported by the National Natural Science Foundation of China (Grant No. 51275558), National Key Science and Technology Research Program of China (Grant No. 2014ZX04015-021), and Shanghai Rising-Star Program (Grant No. 13QA1402100).

References

Abellan-Nebot, J. V., Liu, J., Subirón, F. R., & Shi, J. (2012). State space modeling of variation propagation in multistation machining processes considering machining-induced variations. *Journal of Manufacturing Science and Engineering, 134*(2). 021002–021002.

Bai, D., & Yun, H. (1996). Optimal allocation of inspection effort in a serial multistage production system. *Computers & Industrial Engineering, 30*(3), 387–396.

Cai, W., Hu, S. J., & Yuan, J. (1997). A variational method of robust fixture configuration design for 3-d workpieces. *Journal of Manufacturing Science and Engineering, 119*(4), 593–602.

Camelio, J. A., Hu, S. J., & Ceglarek, D. (2004). Impact of fixture design on sheet metal assembly variation. *Journal of Manufacturing Systems, 23*(3), 182–193.

Cao, Y., Subramaniam, V., & Chen, R. (2012). Performance evaluation and enhancement of multistage manufacturing systems with rework loops. *Computers & Industrial Engineering, 62*, 161–176.

Craig, J. J. (2004). *Introduction to robotics: Mechanics and control*. Prentice Hall.

Ding, Y., Ceglarek, D., & Shi, J. (2002). Design evaluation of multi-station assembly processes by using state space approach. *Journal of Mechanical Design, 124*, 408.

Djurdjanovic, D., & Ni, J. (2001). Linear state space modeling of dimensional machining errors. *Transactions-North American Manufacturing Research Institution of SME*, 541–548.

Du, S., Huang, D., & Lv, J. (2013). Recognition of concurrent control chart patterns using wavelet transform decomposition and multiclass support vector machines. *Computers & Industrial Engineering, 66*, 683–695.

Du, S., & Lv, J. (2013). Minimal Euclidean distance chart based on support vector regression for monitoring mean shifts of auto-correlated processes. *International Journal of Production Economics, 141*, 377–387.

Du, S., Lv, J., & Xi, L. (2012). On-line classifying process mean shifts in multivariate control charts based on multiclass support vector machines. *International Journal of Production Research, 50*, 6288–6310.

Du, S., Xi, L., Ni, J., Pan, E., & Liu, C. R. (2008). Product lifecycle-oriented quality and productivity improvement based on stream of variation methodology. *Computers in Industry, 59*(2), 180–192.

Du, S., Yao, X., & Huang, D. (2015). Engineering model-based bayesian monitoring of ramp-up phase of multistage manufacturing process. *International Journal of Production Research*. http://dx.doi.org/10.1080/00207543.2015.1005247.

Huang, Q., & Shi, J. (2004a). Variation transmission analysis and diagnosis of multi-operational machining processes. *IIE Transactions, 36*(9), 807–815.

Huang, Q., & Shi, J. (2004b). Stream of variation modeling and analysis of serial-parallel multistage manufacturing systems. *Journal of Manufacturing Science and Engineering, 126*, 8.

Huang, Q., Shi, J., & Yuan, J. (2003). Part dimensional error and its propagation modeling in multi-operational machining processes. *Journal of Manufacturing Science and Engineering, 125*(2), 255–262.

Jin, J., & Shi, J. (1999). State space modeling of sheet metal assembly for dimensional control. *Journal of Manufacturing Science and Engineering, 121*(4), 7.

Loose, J.-P., Zhou, S., & Ceglarek, D. (2007). Kinematic analysis of dimensional variation propagation for multistage machining processes with general fixture layouts. *IEEE Transactions on Automation Science and Engineering, 4*(2), 141–152.

Loose, J.-P., Zhou, Q., Zhou, S., & Ceglarek, D. (2010). Integrating GD&T into dimensional variation models for multistage machining processes. *International Journal of Production Research, 48*(11), 3129–3149.

Mantripragada, R., & Whitney, D. E. (1999). Modeling and controlling variation propagation in mechanical assemblies using state transition models. *IEEE Transactions on Robotics and Automation, 15*(1), 124–140.

Paul, R. P. (1981). *Robot manipulators: Mathematics, programming, and control. The computer control of robot manipulators*. The MIT Press.

Shetwan, A. L. G., Vilentin, I. V., & Tjahjono, B. (2011). Allocation of quality control stations in multistage manufacturing systems. *Computers & Industrial Engineering, 60*, 473–484.

Shi, J. (2006). *Stream of variation modeling and analysis for multistage manufacturing processes*. New York: CRC Press.

Shi, J., & Zhou, S. (2009). Quality control and improvement for multistage systems: A survey. *IIE Transactions, 41*(9), 744–753.

Zhou, S., Huang, Q., & Shi, J. (2003). State space modeling of dimensional variation propagation in multistage machining process using differential motion vectors. *IEEE Transactions on Robotics and Automation, 19*(2), 296–309.